Origin of Conductivity Threshold in the Solid Electrolyte Glass System: $(Ag_2S)_x(As_2S_3)_{1-x}$

Chad Holbrook, Ping Chen, D. I. Novita, and P. Boolchand

***Abstract*—The electrical conductivity of $(Ag_2S)_x(As_2S_3)_{1-x}$ glasses increases to display a step-like jump of nearly five orders of magnitude in the narrow composition range, $9\% < x < 15\%$ range. To elucidate the origin of this threshold behavior, we have now examined the molecular structure of these glasses in modulated-differential scanning calorimetry (MDSC) and Raman scattering experiments. Our MDSC results reveal bimodal glass transition temperatures (T_gs), a low-T_g and a high-T_g in the $7\% < x < 40\%$ range but unimodal ones outside this range. The low-T_g phase bears a similarity to that of the stoichiometric glass at $x = 1/2$, or $AgAsS_2$, and we identify it with a Ag-rich phase formed in these glasses once $x > 7\%$. The Ag-rich phase is thought to percolate near $x \sim 9\%$, and to contribute to the large jump in conductivity of the glasses. The high-T_g phase represents a semiconducting As_2S_3 glass phase alloyed with a few mole percent of Ag_2S, and it displays a reversibility window in the $8\% < x < 13\%$ range. The semiconducting phase becomes elastically flexible once $x > 13\%$. Softening of the high-T_g phase lowers Ag^+ ion migration energies and also contributes to the conductivity threshold.**

***Index Terms*—Macroscopic phase separation, modulated DSC, Raman scattering, self-organization, solid electrolyte glasses.**

I. Introduction

ADDITION of the solid electrolytes, Ag_2S, Ag_2Se, and AgI to base oxide- and/or chalcogenide glasses has been examined for the past two decades. Interest in these materials stems from their increased ionic conductivity [1] with progressive alloying of the solid electrolyte additive. Solid electrolyte glasses have found applications as sensors, as electrolytes for batteries, and as materials for electrochromic displays [2]. At a basic level, the increase in conductivity with chemical composition continues to be a subject of ongoing discussions in the field. In some cases, the conductivity displays a gradual increase [3] with the solid electrolyte content. In other cases, one observes [4] a threshold reminiscent of a percolative behavior. In spite of these details, one continues to remain uncertain over the nature of the percolating species. The present glass system has received particular attention in this respect, and evidence [1], [5] of a giant increase of conductivity has been observed when x increases to $\sim 15\%$ as shown in Fig. 1. At $x \sim 5\%$, the electrical conductivity is characteristic of a semiconducting glass, while at $x > 15\%$, it is representative of an ionic conductor.

Manuscript received August 31, 2006; revised April 9, 2007. This work was supported by the U.S. National Science Foundation under Grant DMR-101808 and Grant 0456472. The review of this paper was arranged by Associate Editor A. Bose.

The authors are with the Department of ECECS, University of Cincinnati, Cincinnati, OH 45221-0030 USA (e-mail holbrocm@e-mail.uc.edu; chenpg@ececs.uc.edu; novitadi@ececs.uc.edu; pboolcha@ececs.uc.edu).

Color versions of one or more of the figures in this paper are available online at http://ieeexplore.ieee.org.

Digital Object Identifier 10.1109/TNANO.2007.905540

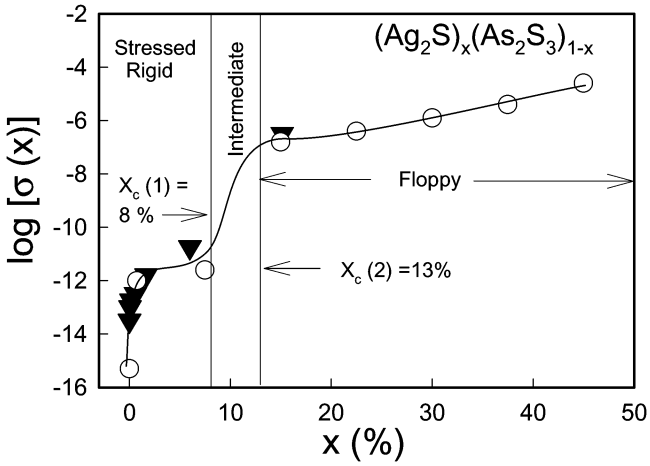

Fig. 1. Electrical conductivity $\sigma(x)$ of titled glasses showing a threshold behavior near $x \sim 0.10$. The open circle ($\circ$) results are taken from [1], while the filled triangle ($\blacktriangledown$) results are from [11]. The three phase identification shown above is inferred from the present work. See text.

Solid electrolytes such as AgI, Ag_2S, Ag_2Se can exist in a glassy phase as additives to base chalcogenide glasses. The realization first emerged [6] from scanning calorimetric measurements that have revealed bimodal glass transition temperatures. In select cases, one T_g comes from the base glass while the other from a Ag-rich glass phase. Theoretical support for these ideas on phase separation have come from constraint counting algorithms that have permitted correlating the magnitude of observed T_gs to the connectedness of the glassy networks [6]. Recently one has found [7] that when Ag is alloyed in S-rich $(x < 1/3)$ Ge_xS_{1-x} glasses, bimodal glass transitions (T_gs) are observed. In these experiments, one of the T_gs near 320 °C is ascribed to an Ag_2S-rich glass phase while the other to the S-deficient base Ge_tS_{1-t} glass phase in analogy to previous work on corresponding selenides [8]. Fundamentally, such macroscopic phase separation is driven by free energy considerations; instead of having a fully polymerized network of a high connectedness and thus high free energies, glasses intrinsically segregate into two separate phases of lower connectedness possessing lower free energies.

Given these ideas on macroscopic phase separation, it is also of interest to inquire when might one of these phases percolate and contribute to a giant conductivity enhancement. Consider, for example, a heterogeneous glass system composed of two glass phases: a conducting one and an insulating one. Imagine steadily increasing the fraction of the conducting phase by chemical alloying. When might one expect conducting glass phase to percolate? The issue was addressed several years ago by H. Scher and R. Zallen [9], who showed that percolation of the minority phase will occur, in general, when its volume

fraction approaches a threshold value of 1/6 or 16.6%. These basic ideas on scalar percolation are relevant to the present work as we will illustrate to understand electrical transport and structure of the present glasses.

The present $(Ag_2S)_x(As_2S_3)_{1-x}$ glass system has been the subject of several previous investigations, including elastic neutron scattering [10], small angle neutron scattering [11], EXAFS [12], Raman scattering [12], field emission SEM [13], and differential scanning calorimetry [11]. In spite of these detailed investigations, a general understanding of features of structure that contribute to the giant enhancement of conductivity in a narrow composition range $10\% < x < 15\%$ of Ag_2S has remained largely elusive. In some of these studies [11], [13], macroscopic phase separation of these glasses was recognized, but the nature of the underlying phases and their role in relation to conductivity enhancement was not obvious.

In the present work we have synthesized $(Ag_2S)_x(As_2S_3)_{1-x}$ glasses over a wide concentration range, $0\% < x < 80\%$, and have examined them in modulated differential scanning calorimetry (MDSC) and Raman scattering experiments. We show that these glasses are intrinsically phase separated on a macroscopic scale in the $8\% < x < 40\%$ range into two bulk glass phases, and such a behavior plays a central role in understanding the giant enhancement of electrical conductivity in the $10\% < x < 15\%$ range. Our results suggest that one of these phases is a Ag-rich phase based largely on the structure of the $x = 50\%$ glass. The second glass phase is the base glass and it is softened by the Ag_2S additive, and it then also contributes to the conductivity enhancement. The rest of the paper is organized as follows. In Section II, we present experimental results. This is followed by Section III in which we discuss these results. A summary of conclusions emerging from the present work is given in Section IV.

II. Experimental

A. Synthesis of Glasses

High purity (99.999%) Ag, S, and As_2S_3 from Cerac Inc., were used as starting materials to synthesize the glasses. Elemental Ag was heated in air to 550 °C to remove traces of surface oxidation. Ag and S were first reacted in evacuated (2×10^{-7} torr) quartz ampoules to synthesize crystalline Ag_2S. The product displayed the characteristic $\beta \longrightarrow \alpha$ crystalline phase transition onset near 175 °C in harmony with published reports [14]. Ag_2S and As_2S_3 were then mixed in the appropriate ratios by weight to prepare bulk glasses of the desired composition x. The starting materials were reacted at 950 °C for 48 h, and melt temperatures were then lowered to 50 °C above the liquidus for several hours before a water quench. Once synthesized glasses were stored in evacuated pyrex tubings. All sample handling was performed in a glove box purged with dry nitrogen gas.

B. Modulated DSC Results

A model 2920 Temperature Modulating DSC (MDSC) from TA Instruments Inc. was used to establish glass transition properties. All scans mentioned in this work were taken at a 3 °C/min scan rate and 1 °C/100 s modulation rate. Typically a sample was heated starting 50 °C below T_g, and taken up in temperature to 50 °C above T_g. The temperature of the calorimeter was then lowered to the starting temperature to record all the heat flow signals in a cool down past the glass transition. The advantage [15] of MDSC over conventional DSC is that it is a far more sensitive instrument and it permits deconvoluting the heat flow endotherm into a reversing and a nonreversing component. Glass transition temperatures (T_gs) are precisely determined from the inflection point of the reversing heat flow. The nonreversing enthalpy (ΔH_{nr}) associated with T_g is deduced by integrating the area under the Gaussian-like peak observed in the nonreversing heat flow signal. A frequency correction [16] to the nonreversing enthalpy ΔH_{nr} is made by subtracting the ΔH_{nr} term measured upon cool down from the term measured upon heating.

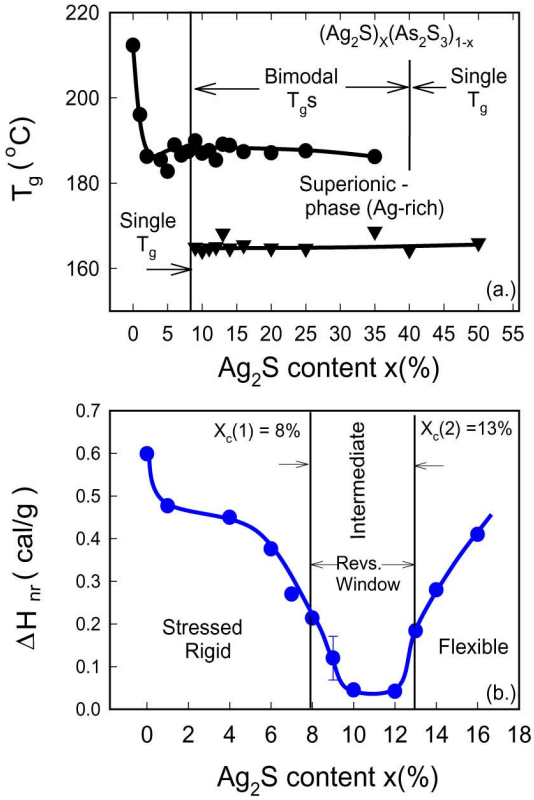

Fig. 2. Compositional variations of: (a) glass transition temperature $T_g(x)$ and (b) the nonreversing enthalpy $\Delta H_{nr}(x)$ in titled glasses. Single T_gs are observed at $x < 8\%$ and at $x > 40\%$, but two T_gs appear in the $8\% < x < 40\%$ intervening region. The global minimum in $\Delta H_{nr}(x)$ serves to define the intermediate phase of the high-T_g phase.

A summary of MDSC results appears in Fig. 2. In general, a solitary T_g is observed at $x < 7\%$, but two T_gs are observed in the $7\% < x < 40\%$ range, followed by a single T_g at higher $x(> 40\%)$. We note that there is a sharp reduction in the value of glass transition temperature of the semiconducting (high-T_g) phase upon alloying a few percent of Ag_2S. Thereafter, T_gs of this phase more or less saturate to a value of about 186 °C independent of x. The T_g of the low-T_g phase remains more or less independent of x and has a value of 168 °C. In Fig. 2(b), we summarize compositional trends in the $\Delta H_{nr}(x)$ term, and find evidence of a global minimum in the $8\% < x < 13\%$ range. Such minima have been observed earlier in chalcogenide glasses and are known to represent the reversibility window [17], [18]. In these windows glass transitions become thermally reversing in character, a feature that is identified with self-organized networks [18] as we shall discuss later.

Glass forming tendency in the present ternary extends up to $x \sim 75\%$. The chemical composition $x = 50\%$ corresponds to the stoichiometric composition $AgAsS_2$, which is also known to exist as a crystalline compound known as Smithite [12]. The stoichiometric composition can be readily vitrified. We have synthesized the $x = 50\%$ glass and have obtained a T_g of 166 °C. We note that this value of T_g is characteristic of the low-T_g phase present in the ternary glasses once x exceeds approximately 10% [Fig. 2(a)].

The specific heat jump near T_g provides in good measure the concentration of a glass phase. The specific heat jump (ΔC_p) at the glass transition for both the low-T_g and high-T_g phases were measured by analyzing the reversing heat flow signals. From MDSC scans, we measure ΔC_p (low-T_g) and ΔC_p (high-T_g) and obtain the ratio R defined as

$$R = \frac{\Delta C_p \text{ (low-}T_g\text{)}}{[\Delta C_p \text{ (low-}T_g\text{)} + \Delta C_p \text{ (high-}T_g\text{)}]}. \tag{1a}$$

The quantity R provides a measure of the fraction of the low-T_g phase in the glasses. We note that the fraction $R(x)$ is vanishing at $x = 7\%$, but it increases sharply in the $7\% < x < 9\%$ range. A plateau sets in the $9\% < x < 13\%$ range. Thereafter, $R(x)$ increases linearly to acquire a value of 100% near $x = 40\%$. We have also measured the molar volumes (V_m) of glasses, and find V_m $(g - As_2S_3) = 16.0$ cm^3/mol and V_m $(g - AgAsS_2) = 14.74$ cm^3/mol. Using these data we have calculated the volume fraction, V(x), of the low-T_g phase using the relation (1b),

$$\text{V(x)} = \frac{A}{B} \tag{1b}$$

where

$$A = \Delta C_p(\text{low-}T_g)V_m(g\text{-}AgAsS_2),$$
and
$$B = [\Delta C_p(\text{low-}T_g)V_m(g\text{-}AgAsS_2) + \Delta C_p(\text{high-}T_g)V_m(g\text{-}As_2S_3)].$$

A plot of V(x) appears in Fig. 3. One finds that in the composition range of $8\% < x < 13\%$, corresponding to the reversibility window, V(x) takes on a value of about 16% and remains unchanged. An enlarged view of the rectangular region of Fig. 3(a) is displayed in Fig. 3(b). The threshold compositions, $x_c(1)$ and $x_c(2)$, represent respectively the stress- and rigidity-transition. Also shown in Fig. 3(b) is the special composition $x = x_{SZ} = 9\%$ where V(x) acquires a value of 16%, the Scher-Zallen threshold [9]. At $x > x_{SZ}$, one expects the low-T_g phase to percolate and electrical conductivity to abruptly increase. We shall return to discuss these results in Section III.

C. Raman Scattering

A Thermo–Nicolet FTIR Research grade bench with a Raman module was used to record FT-Raman spectra of glass samples. An advantage of exciting the scattering in the red instead of the visible light is that one can minimize photostructural effects [19] associated with Ag- photodiffusion in these Ag-bearing glasses. The 1.06 μm laser beam was brought to a loose focus (50 μm spot size) on samples. In these experiments the incoming beam comes to a line focus on samples because of the cylindrical shape of the quartz tubing encapsulating them. Such geometry

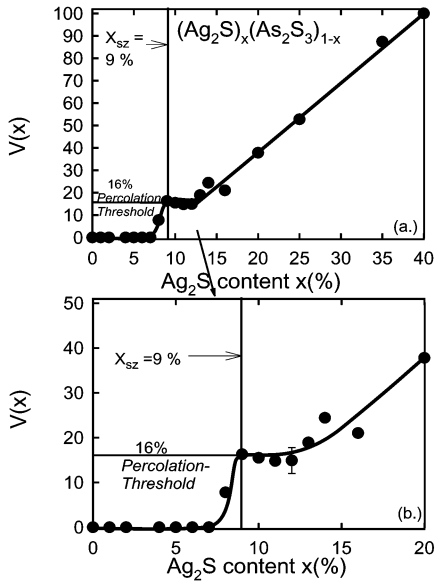

Fig. 3. (a) Plot of V(x), volume fraction of the low-T_g glass phase. It displays a general increase as the Ag_2S content increases in the present $(Ag_2S)_x(As_2S_3)_{1-x}$ glasses. (b) Magnified view of the rectangular region of (a). It shows the V(x) to approach the Scher–Zallen value of 16% when the glass composition acquires a value of $x = 9\%$. See text for details.

further lowers, substantially, the laser power density on samples. The typical power used in these experiments was 100 mW, and an acquisition used 300 cycles resulting in an instrumental resolution of 1 cm^{-1}. At these low power densities, we could not detect any light-induced effects. The observed lineshapes are thought to represent the intrinsic vibrational density of states in the glasses.

Fig. 4 provides a summary of the Raman scattering results on the present glasses displayed systematically with increasing Ag_2S content x. The observed lineshape of a glass sample at $x = 10\%$ is found to be quite similar to the one reported [12], [20] for pristine As_2S_3 glass at $x = 0\%$. Several groups have examined [12]. [20] this particular glass and a fairly good understanding of the vibrational modes have emerged from the recent work of Georgiev *et al.* [20] The narrow features near 180 cm^{-1} and 220 cm^{-1} labeled R are identified with Realgar (As_4S_4) molecules. These molecules segregate from the backbone even in the base glass. In the present glasses, with steadily increasing concentration x, we observe two new features in the spectra; Realgar molecules consistently nanoscale phase separate as x increases to 35%. Concomitantly, a broad mode (labeled as S for Smithite) centered near 375 cm^{-1} begins to manifest, and its presence broadens the main band centered near 350 cm^{-1} of As_2S_3 glass. At $x > 35\%$, the Smithite-mode manifests as a shoulder to the 350 cm^{-1} band. At $x = 50\%$, it becomes the principal feature of the present ternary glasses.

Broadly speaking, features observed in Raman scattering of the present glasses in the 150 cm^{-1} $< \nu <$ 500 cm^{-1} range, largely emerge from vibrations associated with As–S bonds. Scattering from Ag–S bonds is not only much weaker in strength but also it is shifted to lower frequencies (< 150 cm^{-1}). Several groups [5]. [12] have reported Raman scattering of the stoichiometric $AgAsS_2$ glass. Our result for the stoichiometric glass $(x = 50\%)$ in Fig. 4 is in harmony with these earlier reports. The main feature at 375 cm^{-1} in the stoichiometric glass can readily

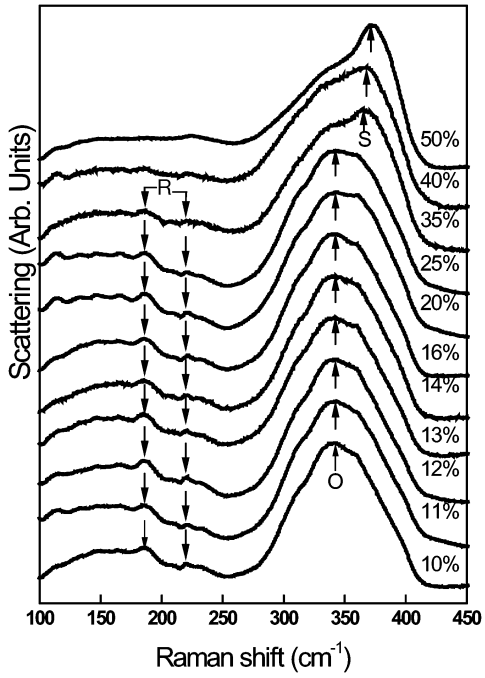

Fig. 4. Raman scattering in $(Ag_2S)_x(As_2S_3)_{1-x}$ glasses at indicated glass compositions x. The mode labeled S near 375 cm^{-1} is characteristic of the 50% glass. This mode is observed in glasses at $x = 25\%, 35\%, 50\%$. It contributes to the high frequency shoulder of the main band centered near 350 cm^{-1}. The main band comes from Orpiment-like phase (O) of the base glass composed of 12-membered rings. The modes near 180 to 250 cm^{-1} labeled R come from As_4S_4 molecules characteristic of Realgar [20].

be identified [5] with the symmetric stretch of As–S modes in AsS_3 pyramids present in 6-membered rings. A 6-membered ring is made up of 3 pyramidal units. The main band in As_2S_3 glass is observed near 350 cm^{-1}, i.e., it is shifted to a lower frequency. We believe this shift comes from AsS_3 pyramids present in rings that have 12 members or 6 AsS_3 pyramids. The blue shift of the mode in question with decreasing ring size is a fairly general feature observed in other glass systems [16]. The blue shift is due to pyramids becoming more stressed in rings of a smaller size as intramolecular interactions grow at the expense of intermolecular ones.

We have also examined Raman scattering from c-$AgAsS_2$ (Smithite) as a function of increasing laser power density. In these experiments, we are able to observe the vibrational modes to steadily broaden and to acquire features characteristic of the glass as the laser power density increases. Light-induced vitrification of Smithite illustrates that the spectrum of the glass (in Fig. 4) evolves smoothly and almost continuously from that of the crystal. These results will be presented elsewhere. Next we shall discuss the structure implications of the Raman scattering and MDSC results next.

III. Discussion

There is broad recognition that Ag in glasses readily photodiffuses [21]. Indeed, applications of spectroscopies that use a beam of visible light or an electron beam to probe structure of Ag-based glasses has always been problematic; one runs the risk of altering Ag-centered local structures in the very process of probing them if the flux of incident beam is high. These limitations are much less severe in using thermal methods to probe glass structure. It is in this respect that MDSC serves as an important check on interpretation of results from more traditional techniques. Use of MDSC as a probe of glass structure through measurements of the reversing heat flow (related to ergodic processes and thermodynamic parameters such as T_g and ΔC_p) and the nonreversing enthalpy (nonergodic processes related to structural arrest) has proved to be quite rewarding as discussed in recent reviews [18], [22]. In DSC experiments one is forced to use higher scan rates (20 K/min) than in MDSC ones (3 K/min) because of the lower sensitivity of the former (dc) versus the latter (ac) method. This limitation leads to kinetic shifts in the glass transition temperature in the former but not the latter method. Furthermore, in DSC experiments one infers T_g and ΔC_p from the total heat flow. This has the obvious limitation that ergodic processes that control these thermodynamic parameters are polluted by nonergodic ones.

A. Macroscopic Phase Separation of $(Ag_2S)_x(As_2S_3)_{1-x}$ Glasses

The bimodal glass transition temperatures observed in the present work (Fig. 2) confirm the earlier findings of Bychkov *et al.* [11] that the present glasses, in the $7\% < x < 25\%$ composition range, are segregated on a macroscopic scale. Macroscopic phase separation of glasses in this composition range is independently corroborated by small angle neutron scattering results [11] which reveal two orders of magnitude higher scattering at $q = 0.002$ A^{-1} in a glass at $x = 16.6\%$ than at $x = 1.8\%$ or even at $x = 37.5\%$. A detailed comparison of compositional variations in T_g of the two phases is summarized in Fig. 2(a). These results are quite similar to those reported earlier [11]. Small differences in T_g trends between the present results and those of Bychkov [11], most likely, result from the use of MDSC by us and DSC by them. For example, in the present work the region of bimodal glass transition temperatures $(7\% < x < 40\%)$ is wider than the one reported by Bychkov [11] $(8\% < x < 25\%)$.

B. Identification of the High-T_g Phase

The high-T_g phase represents the base semiconducting As_2S_3 glass alloyed with a few mole percent of the Ag_2S additive. The sharp drop in T_g of this phase probably comes from weaker Ag–S bonds replacing stronger As–S bonds as Ag replaces As in the backbone interior with a coordination number of 3. Some of the Ag probably also segregates to internal surfaces of the glass to be fourfold coordinated with three bridging S near neighbors forming part of the backbone and a nonbridging S^- thio unit as a dangling end. Ag has a covalent radius of 1.34 A, which is about 12% larger than that of As (1.20 A). The free energy of the alloyed glass will be lowered by segregation of the oversized cation to internal surfaces. Such a fourfold coordination could be compatible with the neutron scattering results of Penfold and Salmon [10] who claim to find evidence for fourfold coordinated Ag at $x = 9.6\%$. The diffraction result must be treated with caution because a ternary glass at $x = 9.6\%$ was treated by Penfold and Salmon as a homogeneous glass with a T_g of 180 °C.

C. Identification of the Low-T_g Phase

The low-T_g phase first nucleates once $x > 7\%$, and it grows precipitously with increasing concentration of Ag_2S. Its T_g then becomes quite similar to that of the stoichiometric glass at $x =$

50%. Once x approaches about 8%, the Ag_2S additive nucleates a Ag-rich low-T_g glass phase instead of alloying in the base glass (high-T_g) phase. We suppose this is the case because replacement of As by the oversized Ag leads to accumulation of strain. On the other hand, macroscopic phase separation lowers the free energy by creating two types of glass phases that are optimally connected. Once the low-T_g phase nucleates, it appears that some of the Ag from the (stressed) high-T_g phase moves over to the low-T_g phase. The signature of this shift of Ag to the high-T_g phase is the mild increase of T_g of that phase once $x > 5\%$. The observation of a low T_g glass transition once $x > 7\%$ suggests that the spatial extent of the Ag-rich phase must be in the micrometer range. And it is possible that at $x < 7\%$, a precursor to the low T_g phase observed (at $x > 7\%$) exists in the present glasses. However, the absence of a low-T_g glass transition at $x < 7\%$ would simply place the spatial extent of such a Ag-rich phase to be less than submicron dimensions.

The structure of Smithite is remarkable in many ways. It is made up of $As(S_{1/2})_3$ pyramids present in 3 membered rings that share 3 Ag^+ compensating cations. The mean coordination number, $\boldsymbol{r}$, of the network can be calculated by taking the coordination numbers of Ag, As, and S to be respectively 3, 3, and 2. Calculations reveal $\boldsymbol{r} = 2.5$, corresponding to the count of Lagrangian constraints due to bond-stretching and bond-bending forces per atom of $n_c = 3.25$. Furthermore, if Ag is mobile in the structure as is suggested from conductivity measurements, then it can be shown that the count of mechanical constraints per atom (n_c) associated with the network reduces to $n_c = 2.50$. The magic value of n_c for the glass forming tendency to be optimized [23] according to J. C. Phillips is $n_c = 3$. It is, therefore, not a surprise that the molecular structure of Smithite lends itself to easy glass formation. The low-T_g glass phase formed in the present glasses near the composition $x = 25\%$, probably consist of rings that are closer to 6 (as in orpiment) rather than 3 as in Smithite. In the $35\% < x < 50\%$ composition range, one may write the approximate chemical stoichiometry of the low-T_g phase to be $(As_2S_3)_x(Ag_2S)_{1-x}$ with x in the $1/3 < x < 1/2$ range. Since both Ag and As are threefold coordinated, the mean coordination number $\boldsymbol{r}$ and therefore T_gs remain largely independent of x. The coordination of Ag of 3 in the Smithite glass is consistent with the neutron scattering results of Penfold and Salmon [10].

D. Conductivity Threshold and Scher–Zallen Percolation of the Low-T_g Phase

The macroscopic segregation of the present ternary glasses into two macroscopically distinct glass phases, has a direct bearing on the conductivity threshold (Fig. 1).As alluded to above, we identify the low-T_g glass phase with an Ag-rich phase. At a basic level, the specific heat increase near T_g when a glass melts provides a measure of the increased degree of freedom available in the molten state compared to the solid glass state. In the present case, the specific heat jump, ΔC_p, provides a means to ascertain the degree of phase separation by directly relating it to the fraction of the two glass phases present. The volume fraction of the low-T_g phase V(x), deduced by analyzing the reversing heat flow signal, is vanishing at $x < 7\%$, but the fraction increases rapidly once $x > 7\%$. The fraction V(x) approaches the threshold value of $\sim$ 1/6 near a glass composition $x = 9\%$ [Fig. 3(b)]. According to Scher and Zallen [9], once the volume fraction of the minority (Ag-rich) phase acquires the threshold value of 16.6%, one expects that phase to percolate. A ternary glass at $x > 9\%$ will be electrically shorted by the low-T_g glass phase, and one expects the electrical conductivity to increase precipitously. Unfortunately, conductivity results in the critical region, $8\% < x < 15\%$ are few and far between. The available results certainly suggest that a large jump in electrical conductivity is taking place once $x > 10\%$. Thus, a central finding of the present work is that a volume-percolation of the Ag-rich low-T_g glass phase most likely contributes to the giant enhancement in electrical conductivity observed once x exceeds 10%.

E. Conductivity Threshold, Ag Tracer Diffusion, and Reversibility Window of the High-T_g Phase

The molecular structure of the base As_2S_3 glass has been the subject of numerous previous studies [12], [20]. The stoichiometric glass has often been modeled after its crystalline counterpart: orpiment $(c - As_2S_3)$ to consist of a fully polymerized network of S bridging pyramidal $As(S_{1/2})_3$ units. If the picture were as simple as described above, one would expect As_2S_3 glass to be nearly self-organized. Experiments have shown the stoichiometric glass to be stressed-rigid [24]. Detailed examination of Raman scattering [20] and Mössbauer spectroscopy [25] results show the glass in neither fully chemically ordered nor fully polymerized. Segregation of Realgar molecules clearly leaves the backbone S-rich. Alloying a few mole percent of Ag_2S in the base glass apparently lowers the connectedness of the backbone as glasses soften to enter the intermediate phase in the composition range $8\% < x < 13\%$ (Fig. 2).

In analogy to earlier results on Chalcogenide glasses [15], [26], observation of the reversibility window permits fixing the *three elastic phases* of the high-T_g phase. In the composition range $9\% < x < 13\%$, the majority phase present in the ternary glasses is the high-T_g phase. Note that V(x) = 25% at $x = 10\%$ as shown from the plot of Fig. 3(b). The observation of a reversibility window suggests that glasses at $x < 8\%$ are stressed-rigid, those at $x > 13\%$ are *flexible*, while those in the *intermediate* composition are *self-organized* [18]. Thus, as the ternary glass composition increases to $x = 13\%$, the high-T_g glass phase becomes elastically flexible. This has the important consequence that diffusion of Ag^+ ions associated with the high-T_g phase becomes facile, since the energy required to elastically deform the network and provide for the oversized Ag^+ ion to diffuse decreases rapidly. Softening of the high-T_g phase assists Ag^+ ion conduction once $x > 13\%$, and also contributes to the conductivity enhancement observed in the present glasses in this composition range (Fig. 1).

Macroscopic segregation of the present ternary glasses in the $8\% < x < 40\%$ range has some consequences for Ag tracer diffusion. One expects Ag^+ ions to display two distinct diffusion constants, one associated with the high-T_g phase and the other with the low-T_g phase. The Ag diffusion in the high-T_g phase would then be expected to increase dramatically as x exceeds $x_c(2) = 13\%$, and glasses enter the *flexible* phase. The available ^{110}Ag tracer diffusion results of Drugov *et al.* [27] broadly support the picture above. Drugov *et al.* find Ag diffusion constant $D = 5 \times 10^{-13} \mathrm{cm}^2/\mathrm{s}$ at $x = 6\%$, but to increase by nearly three orders of magnitude to $D = 10^{-10}$ cm^2/s as x increases to 15%. Unfortunately, the group did not report Ag diffusion in

the region of interest, i.e., $6\% < x < 15\%$, where large scale changes in conductivity are observed.

IV. Conclusion

The molecular structure of the ternary $(Ag_2S)_x(As_2S_3)_{1-x}$ glasses has been examined in MDSC and Raman scattering measurements over a wide composition range, $0 < x < 70\%$. At $x > 7\%$, glasses segregate on a macroscopic scale into an Ag-rich superionic-phase (low-T_g) and a semiconducting (high-T_g) phase. The present MDSC results show that the majority high T_g phase displays a reversibility window in the $8\% < x < 13\%$ range. The observation fixes the three elastic phases in the glasses, with compositions at $x < 8\%$ as *stressed-rigid*, those at $x > 13\%$ as *flexible* while those in the intervening range, $8\% < x < 13\%$, belong to an *intermediate* phase [28]. The latter composition range comprises networks that are stress-free. The threshold behavior in electrical conductivity noted by Borisova *et al.* [1] near $x \sim 10\%$ correlates well with: a) the present identification of the intermediate phase in the $8\% < x < 13\%$ range (as illustrated in Fig. 1) and b) the macroscopic phase separation and subsequent volume percolation of the low T_g Ag-rich superionic-phase. Both features a) and b) are thought to contribute to the giant enhancement in electrical conductivity reported in the present ternary glasses.

References

[1] E. Kazakova and Z. U. Borisova, "Electrocondutivity of $(Ag_2S)_x(As_2S_3)_{1-x}$ glass systems," *Fiz. Khim.Stekla*, vol. 6, pp. 424–427, 1980.

[2] K. L. Ngai, J. Habasaki, Y. Hiwatari, and C. Leon, "A combined molecular dynamics simulation, experimental and coupling model study of the ion dynamics in glassy ionic conductors," *J. Phys., Condens. Matter*, vol. 15, pp. S1607–S1632, 2003.

[3] D. L. Sidebottom, "Influence of cation constriction on the ac conductivity dispersion in metaphosphate glasses," *Phys. Rev. B*, vol. 61, pp. 14 507–14 516, 2000.

[4] M. Mangion and G. P. Johari, "Electrical relaxation and aging effect in $AgPO_3$ glass," *Philos. Mag. B-Phys. Condens. Matter Stat. Mech. Electron. Opt. Magn. Properties*, vol. 57, pp. 121–132, 1988.

[5] V. Y. Slivka, Y. M. Vysochanskii, V. A. Stefanovich, V. S. Gerasimenko, and D. V. Chepur, "Some peculiarities of $AgAsS_2$ phonon-spectra," *Fizika Tverdogo Tela*, vol. 24, pp. 696–706, 1982.

[6] P. Boolchand and W. J. Bresser, "Mobile silver ions and glass formation in solid electrolytes," *Nature*, vol. 410, pp. 1070–1073, 2001.

[7] P. Boolchand, F. Wang, U. Vempati, M. Mitkova, and M. Kozicki, "Bimodal T_g and macroscopic phase separation in Ag-Ge-S bulk glasses," *Bull. Amer. Phys. Soc.*, vol. 49, p. 826, 2004.

[8] Y. Wang, M. Mitkova, D. G. Georgiev, S. Mamedov, and P. Boolchand, "Macroscopic phase separation of Se-rich $(x < 1/3)$ ternary $Ag_y(Ge_xSe_{1-x})_{1-y}$ glasses," *J. Phys., Condens. Matter*, vol. 15, pp. S1573–S1584, 2003.

[9] H. Scher and R. Zallen, "Critical density in percolation processes," *J. Chem. Phys.*, vol. 53, pp. 3759–3761, 1970.

[10] I. T. Penfold and P. S. Salmon, "Glass-formation and short-range order in chalcogenide materials—The $(Ag_2S)_x(As_2S_3)1-x(0 <= x <= 1)$ pseudobinary tie line," *Phys. Rev. Lett.*, vol. 64, pp. 2164–2167, 1990.

[11] E. Bychkov, D. L. Price, and A. Lapp, "Universal trend of the haven ratio in glasses: origin and structural evidences from neutron diffraction and small-angle neutron scattering," *J. Non-Crystal. Solids*, vol. 293, pp. 211–219, 2001.

[12] A. T. Steel, G. N. Greaves, A. P. Firth, and A. E. Owen, "Photodissolution of silver in arsenic sulfide films—An Exafs study," *J. Non-Crystal. Solids*, vol. 107, pp. 155–162, 1989.

[13] B. Arcondo, M. A. Urena, A. Piarristeguy, A. Pradel, and M. Fontana, "Homogeneous-inhomogeneous models of $Ag_x(Ge_{0.25}Se_{0.75})_{100-x}$ bulk glasses," *Physica B, Condens. Matter*, vol. 389, pp. 77–82, 2007.

[14] P. Junod, H. Hediger, B. Kilchör, and J. Wullschleger, "Metal-nonmetal transition in silver chalcogenides," *Philos. Mag.*, vol. 36, pp. 941–958, 1977.

[15] D. Selvanathan, W. J. Bresser, and P. Boolchand, "Stiffness transitions in Si_xSe_{1-x} glasses from Raman scattering and temperature-modulated differential scanning calorimetry," *Phys. Rev. B*, vol. 61, pp. 15 061–15 076, 2000.

[16] *Modulated DSC Compendium*. New Castle, DE: TA Instrument, 1997.

[17] S. Chakravarty, D. G. Georgiev, P. Boolchand, and M. Micoulaut, "Ageing, fragility and the reversibility window in bulk alloy glasses," *J. Phys., Condens. Matter*, vol. 17, pp. L1–L7, 2005.

[18] P. Boolchand, D. G. Georgiev, and B. Goodman, "Discovery of the intermediate phase in chalcogenide glasses," *J. Optoelectron. Adv. Mater.*, vol. 3, pp. 703–720, 2001.

[19] H. Fritzsche, "Light-induced structural changes in glasses," in *Insulating and Semiconducting Glasses*, P. Boolch, Ed. Singapore: World Scientific, 2000.

[20] D. G. Georgiev, P. Boolchand, and K. A. Jackson, "Intrinsic nanoscale phase separation of bulk As_2S_3 glass," *Philos. Mag.*, vol. 83, pp. 2941–2953, 2003.

[21] J. Gump, I. Finkler, H. Xia, R. Sooryakumar, W. J. Bresser, and P. Boolchand, "Light-induced giant softening of network glasses observed near the mean-field rigidity transition," *Phys. Rev. Lett.*, vol. 92, 2004.

[22] P. Boolchand, D. G. Georgiev, T. Qu, F. Wang, L. C. Cai, and S. Chakravarty, "Nanoscale phase separation effects near $(\boldsymbol{r})$over-bar $= 2.4$ and 2.67, and rigidity transitions in chalcogenide glasses," *Comptes Rendus Chimie*, vol. 5, pp. 713–724, 2002.

[23] J. C. Phillips, "Structural principles of amorphous and glassy semiconductors," *J. Non-Crystal. Solids*, vol. 35–36, pp. 1157–1165, 1980.

[24] D. Georgiev, "Molecular structure and intermediate phases in Group-V binary chalcogenide glasses," Ph.D., Dept. ECECS, Univ. Cincinnati, Cincinnati, OH, 2003.

[25] I. Zitkovsky and P. Boolchand, "Molecular-Structure of As_2S_3 glass," *J. Non-Crystal. Solids*, vol. 114, pp. 70–72, 1989.

[26] F. Wang, S. Mamedov, P. Boolchand, B. Goodman, and M. Chandrasekhar, "Pressure Raman effects and internal stress in network glasses," *Phys. Rev. B*, vol. 71, pp. 174–201, 2005.

[27] Y. Drugov, V. Tsegelnik, A. Bolotov, Y. Vlasov, and E. Bychkov, "^{110}Ag tracer diffusion study of percolation transition in $Ag_2S - As_2S_3$ glasses," *Solid State Ion.*, vol. 136–137, pp. 1091–1096, 2000.

[28] P. Boolchand, G. Lucovsky, J. C. Phillips, and M. F. Thorpe, "Self-organization and the physics of glassy networks," *Philos. Mag.*, vol. 85, pp. 3823–3838, 2005.

Authors' photographs and biographies not available at the time of publication.